

ENERGY EFFICIENT NANOCELLULOSE SHEETS FOR PRODUCT APPLICATION

Wriju Kargupta¹, Joanne Tanner², Warren Batchelor³.

^{1,2,3}Bioresource Processing Research Institute of Australia, Chemical Engineering Department, Monash University, Clayton, Australia.

ARTICLE INFO

ABSTRACT

Corresponding Author:

Wriju Kargupta¹

Bio resource Processing Research Institute
of Australia, Chemical Engineering
Department, Monash University, Clayton,
Australia, 3800

Email:wriju.kargupta@tutanota.com

Synthetic polymer and plastics which is currently used as barrier material in packaging industry is neither renewable nor biodegradable, creating a serious threat to the ecosystem. Nano cellulose which is obtained by breaking down cellulose fibers into nano scale dimensions, have unique properties with the potential to dramatically impact many commercial markets including packaging. This research investigates refining of cellulose fiber to produce sustainable nano cellulose using laboratory PFI mill and industrial Disc refiner. Refined pulp was made into nano cellulose sheet using standard laboratory paper making technique through vacuum filtration. The tensile index and sheet density for PFI mill refined BEK and Disc refined NBSK showed an approximately five times and two times improvement over unrefined BEK and NBSK pulp respectively highlighting role of refining in improving mechanical structure of nano cellulose sheets. This strength enhancement comes at a cost of 17417 kWh/t specific refining energy in lab scale PFI mill refining and 3346.3 kWh/t specific refining energy in industrial scale Disc refining. Fines generation as a result of refining decreased the porosity by 37.972% and 48.939% in Disc refined NBSK and PFI mill refined BEK respectively which improved the water vapor and oxygen permeability. Refining decreased the water vapor permeability by approximately ten times for both BEK and NBSK making them very comparable with synthetic polymers such as polyethylene (PE). The lowest value of oxygen permeability achieved with PFI mill refined BEK and Disc refined NBSK was 0.533 ± 0.098 and 0.762 ± 0.03 (cc. μ m)/(m².day.kPa) which is very competitive with that of polymers used in plastics. Additionally, the surface roughness decreased by 77.05% and 52.8% for PFI mill refined BEK and Disc refined NBSK respectively which promises refining as an excellent tool to produce smooth

"ENERGY EFFICIENT NANOCELLULOSE SHEETS FOR PRODUCT APPLICATION"

nano cellulose sheets for printed electronics applications.

KEYWORDS: Synthetic polymer; Nanocellulose; packaging industry; laboratory PFI mill; high aspect ratio .

INTRODUCTION

The packaging industry currently uses raw materials which is heavily dependent on fossil fuel derived plastics which raises the concern from both economical and environmental perspective (Ferrer, Pal, and Hubbe 2017; Johansson et al. 2012). Though plastics have high strength and barrier properties, an over dependence and continuous use have raised issues in terms un sustainability, increase in raw material prices and waste disposal problems (Nair et al. 2014) and serious problem on global environment (Kuswandi 2017). Bio based packaging including biodegradable and biocompatible packaging, is an alternative to excessive use of plastics and polymers. The global consumer packaging demand is currently in range of US400b-\$500b, which is one of the fastest growing markets (Nair et al. 2014). Most packaging industries relies on petrochemical based materials such as polyethylene (PE), polypropylene (PP), polystyrene (PS), polyethylene terephthalate (PET) as gas barrier materials (Aulin, Salazar-Alvarez, and Lindström 2012). However, these materials are non-recyclable and non-biodegradable. Nano-cellulose derived from wood materials stands out to be a highly sustainable material having excellent moisture and air barrier performance for applications in food, pharmaceutical and electronic industry(Tharana than 2003).Due to excellent barrier properties, nano-cellulose can also be a potential for replacing plastics in printed electronics application(Hoeng, Denneulin, and Bras 2016; Agate et al. 2018).

Thus, to meet the increasing demand in a sustainable, energy efficient and eco-friendly way cellulose nano-fiber has been a subject of much research. Cellulose is an environmentally friendly, renewable polymer with good mechanical properties, cheap and abundant. When cellulose is refined or homogenised at high pressure it gives rise to very low diameter, high aspect ratio nano-cellulose fibers (Ang, Haritos, and Batchelor 2019). Nano-cellulose also referred to as Micro fibrillated cellulose (MFC) or Cellulose nano-crystal (CNC) are a new set of material with nano order scale interconnected fibrils and enhanced mechanical

strength (Nakagaito and Yano 2005). Nano-cellulose can be processed into strong films(Sehaqui et al. 2010), membranes(Sehaqui et al. 2012). The use of nano-cellulose as reinforcing agent and bio composites has been also investigated for packaging applications (Youssef, El-Samahy, and Rehim 2012; Tingaut, Zimmermann, and Lopez-Suevos 2010). The potential application of nano-cellulose films includes food packaging, high strength sheets, which is due to its excellent thermal and barrier properties (Lavoine et al. 2012; Li, Mascheroni, and Piergiovanni 2015; Kuswandi 2017).

To enhance mechanical strength and barrier property of nano-composites, nano-cellulose has been either used as a filler or reinforcing agent. For example, (Abdollahi et al. 2013)reported that tensile strength of nano-composite increased from 18.03 to 22.4 MPa with increasing nanocellulose content from 0 to 5 wt.%. The mechanical properties of starch-gelatine-nano-cellulose films were also studied with increase in gelatine and nano-cellulose concentration increasing tensile strength which indicates better film resistance useful for packaging industry(Alves et al. 2015). Bio nano-composite films of carboxy methyl cellulose and starch reinforced with nano-cellulose also claimed to increase of tensile strength with gradual addition of nano-cellulose (El Miri et al. 2015). Nano-cellulose provides a physical barrier in the nano-composite films, creating a tortuous path for moisture permeating across the membrane which increases the effective path length for diffusion, thereby improving barrier properties (Paralikar, Simonsen, and Lombardi 2008; Rhim and Ng 2007). Addition of nano-cellulose as a filler by 3%, 6% and 9% has improved decreasing water vapour permeability by 7%, 20% and 29% respectively(Silvério, Flauzino Neto, and Pasquini 2013). Nano-cellulose have been found to create film impermeability by creating longer diffusion paths for oxygen and water vapor permeation (Belbekhouche et al. 2011).

There has been extensive study on nano-cellulose clay-composites where nano-cellulose strength and barrier properties has been seen to improve water vapour

permeability and tensile strength (Aulin, Salazar-Alvarez, and Lindström 2012; Ho et al. 2012; Thao Ho et al. 2013; Ahmadzadeh et al. 2015; Honorato et al. 2015). Nano-cellulose- montmorillonite (MMT) composites also showed to lower water vapor permeability by 50% with addition of 16.7 wt.% MMT (Garusinghe et al. 2018). However, clay content exceeding 5wt. % decreases composite strength with the formation of large MMT agglomerates (Okada and Usuki 2006). The oxygen barrier properties of nano-cellulose-nano clay bio hybrid films outperformed commercial packaging material with $0.07 \text{ cm}^3\mu\text{m}^2\text{day}^{-1}\text{kPa}^{-1}$ reported for pure nano-cellulose films (Aulin, Salazar-Alvarez, and Lindström 2012).

The processes by which nano cellulose can be processed into films are by vacuum filtration (Varanasi and Batchelor 2013), solvent casting, and also by hot pressing (Österberg et al. 2013). However, most of the studies on nano cellulose as barrier material has been focused on bio composites or as a reinforcing agent (Isogai 2013; Aulin, Salazar-Alvarez, and Lindström 2012; Ho et al. 2012). There has been no study reported which has investigated the correlation of refining of nano-cellulose with barrier properties. Refining of cellulose pulp into nano cellulose by PFI mill refining enable an entangled network of nano-fibers which can be useful for barrier properties. Nano-cellulose films were prepared using TEMPO oxidized cellulose nanofibers and oxygen permeability was reported to be $400 \text{ cm}^3\mu\text{m}^2\text{day}^{-1}\text{kPa}^{-1}$ (Fukuzumi et al. 2009) which is an order of magnitude lower than petroleum-based barrier materials like PVC $20\text{--}80 \text{ cm}^3\mu\text{m}^2\text{day}^{-1}\text{kPa}^{-1}$ and PVDC $0.1\text{--}3 \text{ cm}^3\mu\text{m}^2\text{day}^{-1}\text{kPa}^{-1}$ (Lange and Wyser 2003). However, the poor water vapor barrier permeability of pure nano-cellulose film were reported to be $234 \text{ g/m}^2\text{.day}$ (Rodionova et al. 2011). This may be because of high polarity of nano cellulose which attracts water vapor. Thermal treatment has also been explored which decreased water vapor permeability by 50% by heating nano-cellulose film at $175 \text{ }^\circ\text{C}$ for 3 hrs (Sharma et al. 2014). This may be due to increase in hydro phobicity and reduce porosity by heat treatment. Different polymers, polymer blends, and composites are the most widely used

materials in packaging industry which uses unsustainable coatings of wax, plastics or aluminium (Ferrer, Pal, and Hubbe 2017). The use of coating or grafting nanocellulose with polymers or the use of chemical agents to modify nano cellulose structure suffers from the significant drawback of limiting the biodegradability and recyclability of resulting composite.

While these results indicate a promising outlook for nanocellulose as polymer composite reinforcement (Rodionova et al. 2011); uncertainty still exists in how pure nanocellulose film develops for a given amount of mechanical treatment. Thus, controlling the pore size, fines percentage and water vapour transmission rates is critical to engineer and design good packaging and smooth surface materials. The surface roughness of nano cellulose films were recently engineered to produce smooth surfaces (Shanmugam et al. 2020) by spray coating, however they missed out to highlight the impact of refining levels and subsequent energy consumption which may lead to production of high quality smooth nano cellulose sheets.

Refining is a mechanical treatment to the pulp fibers done to improve the properties of final nano cellulose sheet product. Refining is a mechanical treatment to the pulp fibers done to improve the properties of final nano cellulose sheet product. Mechanical treatment like PFI mill or disk refining works on the principle of subjecting fibers to large shear forces which fibrillate the micro fibrils enhancing the fiber bond ability, and formation of dense structure. This beating process creates delimitation and peeling of cell wall structure of cellulose which increases the specific surface area and also relative bonded area (Stankovská et al. 2019). Fines are small fibers which are generated during refining process where the external and internal cell wall structure are peeled off. In paper and pulp production, different types of pulp fines are generated during refining. Pulp particles that pass through $76 \mu\text{m}$ diameters round hole or a 200-mesh screen are known as fines (Seth 2003; Hyll 2015; Kumar 2012). Fines which are produced at much lower energy level, have much larger specific surface area, aspect ratio, small size than whole pulp and they improve fibre-fibre bond strength,

sheet densification and strength (Seth 2003). This promotes the development of nano-cellulose with high fines percentage which improves fiber entanglement. The understanding of nano-cellulose fiber diameter and its correlation with sheet strength has been well established (Zhang et al. 2012; Ang, Haritos, and Batchelor 2019), however they failed to highlight the significance of pore size distribution and barrier property optimization with energy consumption. Refining also positively influences the density, porosity formation, and sheet strength. With subsequent refining the inner layers are exposed that allows the material to create a dense network which makes them useful as filler, in composites manufacture, and as coating films (Ferrer, Pal, and Hubbe 2017). While numerous studies have been conducted which have focused on tailoring the structure and porosity of nano-cellulose sheets by adding polymer, clay however there has been no studies reported which has tried to develop a trade-off between refining energy and nano-cellulose sheet barrier and surface roughness property development.

MATERIALS AND METHODS

Materials

Lab scale PFI refining

Hardwood BEK pulp was refined using a PFI mill, Model No 164 at Monash University, BioPRIA, according to TAPPI standard 248 (TAPPI 2001a). Pulp at a solids content of approximately 10 wt.% was refined at 15,000, 30,000 and 50,000 revolutions, and the refined samples were designated as BEK 15k, BEK 30k and BEK 50k, respectively (Table 2). After PFI refining, the samples were diluted to 1.2 wt. % solids and disintegrated for 15,000 revolutions in a 3 L Mavis Engineering standard disintegrator, Model No 8522, and used for sheet production.

INDUSTRIAL SCALE MECHANICAL REFINING

Softwood NBSK pulp was refined in a 14-inch single disc LC Aikawa low consistency disc refiner located at The University of British Columbia (UBC). The UBC disc

refiner is powered by a 112-kW motor. It uses a 30-kW centrifugal pump. Softwood pulp was refined to various levels in this disc refiner at a constant feed flow rate of 250 L/min and a consistency of 3.6 wt%. The stock was recirculated until the desired energy input was reached. The specific edge load (SEL) was maintained at 0.6 J/m with a plate of bar edge length 2.74 km/rev operating with a horizontal rotational speed of 1200 rpm. All the operational refining parameters (flow rate readings, pressure, temperature indicator, gap clearance indicator, valve opening, pump frequency reading and refiner speed) were controlled using a computer interface (Lab VIEW program). The resulting fibers were labeled in order of increasing degree of refining from NBSK0 (unrefined) to NBSK11.

INDUSTRIAL SCALE SPECIFIC ENERGY CONSUMPTION

The power of the UBC disc refiner was recorded by Lab VIEW software, where net power (P_{net}) is the total power used by the refiner motors minus the no-load power (water flowing through the refiner). The specific energy consumption (SEC) measurement is then calculated as in (Eq 1). Specific edge load (SEL), which is a measure of fibre treatment intensity, is calculated as the ratio of net power to the product of bar edge length (BEL) and motor rotational frequency (Eq 2).

$$SEC = \frac{P_{net}}{m} \dots \dots \dots (1)$$

where P_{net} is net power consumption in (kW), and m is mass flow rate of dry fibres through refiners in (tonnes/hour).

$$SEL = \frac{P_{net}}{BEL * (RPM/60)} \dots \dots \dots (2)$$

where SEL is in J/m; P_{net} is in kW; BEL (product of number of rotor and stator bars and contact length of opposite bars) is in km/rev; and RPM is the refiner motor frequency in revolutions per minute. The naming conventions, and treatment types for each sample produced in this study are summarized in Table 3.

Table 2: BEK fiber sample naming convention and treatment type

Sample	PFI revolutions	milling
BEK0	0	
BEK15k	15,000	
BEK30k	30,000	
BEK50k	50,000	

Table 3: NBSK fiber sample naming convention and treatment type.

Sample	Refining time in Disc Refiner, seconds
NBSK0	0
NBSK4	1260
NBSK6	1869
NBSK11	3959

BRECHT-HOLL FIBER CLASSIFICATION (SCREENING)

An equivalent dry weight of 1-2 gm was taken from wet BEK pulp (10-12 wt.%) and wet NBSK pulp (1-3.5 wt.%). The subsamples were diluted with water (≤ 1 wt.%) and mixed with Waring Commercial Immersion blender (WSB 33XNNA) for 1 minute. Samples were classified using a Brecht-Holl 200 mesh screen. A dilution water flow rate of 2 L/min was maintained during classification and a water sparge was used to agitate the sample. A very diluted solids consistency of ≤ 1 wt.% was maintained to avoid clogging of the mesh screen and sufficient jet flow velocity was supplied to ensure adequate fiber separation and minimise floc formation. Due to the high volume of water associated with the fines fraction, it is challenging to separate and quantify fines (Fischer et al. 2017). Hence long fibers were quantified

in these trials. The coarse rejects, which did not pass through the mesh, were collected, dried and quantified. Where required, the screened fines fraction was quantified by difference.

LABORATORY HANDSHEET MAKING

All samples were disintegrated for 15,000 revolutions in a 3 L Mavis Engineering Standard Disintegrator (Model 8522). All hand sheets were prepared using a British Hand sheet Maker (Model 8802). A 60 gsm hand sheet was formed from 600 mL of a 0.2 wt.% suspension using GE What man Grade 541 filter paper (22 μ m pore size) placed on a 150 mesh (104 μ m pore size). Drainage time was measured and recorded from the start of automated drain cycle until the sheet was completely drained. Drained sheets were couched manually with blotting paper and carefully separated from the mesh and original filter paper. Sheets were then pressed at 345 kPa for 5 min in an automatic L&W sheet press (A B Lorentzen & Wettre, Model No 576). 3 circular hand sheet replicates were produced for each fiber sample and sheets were maintained at constant conditions (50 % relative humidity, 23 °C according to TAPPI T402 standards (TAPPI 2001b) for 24 hours prior to testing.

HANDSHEET PROPERTY MEASUREMENTS

Mechanical properties

The dried sheets were then collected and dried at 105°C in a Thermo line BTC-9090 oven to determine the sheet grammage and density. Hand sheets were cut into 15 mm wide strips using a sheet cutter (Delta Hydraulics CT01861B). Stress-strain load to fracture measurements. Stress strain load to fracture measurements were performed for each sample using an Instron Model 5566 Universal Testing Machine with a 10 mm/min extension rate. At least 15 separate 10 cm strips from 3 replicate hand sheets were measured for each fiber sample for each refining level. Force (N) vs elongation at break (mm) was recorded. The strength results were expressed as tensile index, which was calculated by dividing the maximum tensile load (load at break) by the width of the strip (15 mm) and grammage of

paper sheet (60 g/m²). The mean sheet thickness was measured as an average of 20 random points for each sheet using descriptive statistics in a Lorentzen &Wettré L&W Micrometer (Model No 51). The sheet density was evaluated by dividing basis weight by mean thickness of the sheets.

BARRIER PROPERTIES

Air Permeance

An L&W air permeance tester with an operating range from 0.003 to 100 µm/Pa.S was used to measure air permeance of unrefined sheets. Two replicates were tested for each sheet.

Water Vapour Permeability: The water vapor transmission rate of the unrefined and refined NBSK and BEK sheets were measured at 23°C and 50% relative humidity by following ASTM E96, using desiccant method (E96/E96M-16 2016). The sheets were then pre-dried at 105°C in a Thermoline BTC-9090 for at least 4 hrs. The 63.5 mm diameter cups complying with the standard were filled with dried calcium chloride (desiccant) and sealed with the test sample. This arrangement was kept in humidity condition chamber and variation in mass of the permeability cups over time was recorded at regular intervals of 4hrs over a span of 2-3 days. The slope of the trend line of increase in mass over time gives the rate of change in mass which quantifies water vapor transmission rate (WVTR). The WVTR was then normalized by thickness of paper to determine water vapour permeability (WVP). The thickness of sheets (unrefined and refined) was measured using L&W thickness tester.

MIP porosimeter

The sheet pore size distribution was measured using a Micro meritics' Auto Pore IV 9500 series. This technique quantifies a material's pore size distribution and porosity by applying increasing pressures (up to 60,000 psia) to a sample immersed in mercury and recording the volume of mercury intruded into pores. Samples were cut into approximately 5 mm × 5 mm small pieces and degassed for at least two days prior to characterization. A penetrometer with 0.412 mL stem volume was used to carry out the measurements. After degassing, approximately 0.1 g of

sample was placed in the penetrometer and the analysis conducted. The volume of mercury intruded into pores is converted to equivalent pore sizes using the instrument software(Giesche 2006).

Porosity calculation: The sheet density was calculated by dividing the basis weight with mean thickness. The apparent porosity of the sheet was determined from Eq (1) by adapting the density of cellulose (1500 kg/m³ for nano cellulose) and pulp fibers sheet density was measured (Sim and Youn 2016).

$$\text{Porosity (\%)} = \left(1 - \frac{\text{sheet density}}{\text{cellulose density}}\right) * 100 \dots (1)$$

Oxygen permeability: The oxygen transmission rate (OTR) through the refined nano cellulose sheet was determined according to the ASTM standard F1927 using an Ox-Tran 2/22 oxygen transmission rate tester (Mocon) (ASTM 1927). The test area of the sample was 50 cm². The tests were carried out at 23 °C and 50% relative humidity's using 100% oxygen as a test gas. The OTR was multiplied by the thickness of the film, and the corresponding oxygen permeability (OP) was reported.

FIBER AND SHEET CHARACTERISATION

The microscopic morphology of iridium coated air-dried fiber (0.001 wt.%) samples was determined using Nova Nano SEM 450 FEG at an accelerating voltage of 5 kV. The unrefined fibers were taken at a lower magnification of 200X -500X, and refined fibres were taken at higher magnification of 50,000X to capture all the image. The image pixels were then calibrated with length scale using Image J software and around 200 observable fibres were counted manually. This was followed by sorting the nano cellulose (both BEK & NBSK samples) into 10 nm sized bins and then plotted and compared on a frequency versus bin range graph to show effect of refining on fiber diameter. The macroscopic morphology of sheets (259 µm x 259 µm area of both rough and smooth sides) was determined using optical pro filometer (OLS5000, Olympus, Japan) with a 50X objective. The nano cellulose sheets peeled from stainless steel side was the smooth side and side which was

exposed to drying and blotting paper is referred as rough side. The average aerial roughness (S_a) and root mean square roughness (S_q) of both rough and smooth side were determined in triplicates. Effect of refining on optical properties of sheets was determined by using Agilent Cary 60 UV-vis Spectrophotometer in the wavelength ranging between 200-800 nm.

RESULTS

Specific energy consumption (SEC)

The specific energy consumption for BEK and NBSK pulp samples refined by lab PFI mill and industrial disc refiner are summarized in Eq4a and Eq 4b respectively (Fig S1 a and Fig S1 b). The most highly processed lab refined sample, BEK50k, showed the highest energy consumption of 17417 kWh/t. With increasing PFI mill revolutions; there is increase in SEC for both BEK and NBSK sample. NBSK 11 which is most heavily disc refined sample showed highest specific energy consumption of 3346 kWh/t. The specific energy consumption measured in lab scale was the average of three replicates and standard deviation was (3.5-4) % for different refining levels. However, disc refining was conducted once, and no replication studies were conducted.

It is worth noting that in PFI mill the measured energy consumption was 0.37 kWh/tonne/rev for BEK pulp (Eq 4a, Fig S1a) and that of NBSK pulp is 0.846 kWh/t/s

$$E_{PFI} = 0.37 r \dots \text{(Eq 4a)}$$

Where E_{PFI} is Specific energy consumption of PFI mill refiner (kWh/t) and r is refining level (PFI mill revolutions $\times 10^3$)

$$E_{disc} = 0.846 t \dots \text{(Eq 4b)}$$

Where E_{disc} is Specific energy consumption of disc refiner (kWh/t) and t is disc refining time in seconds.

MECHANICAL PROPERTY

Fig 1 shows the average tensile index, sheet density and drainage time for unrefined, PFI mill and disc refined as a function of specific energy consumption. It is worth noting that the tensile index, sheet density and drainage time values

shown in Fig 1 were calculated as an average of multiple strips taken from 2 handsheets for each sample respectively. From Fig 1 a, all sheets had an approximately twofold and threefold strength improvement in terms of tensile index and sheet density respectively. The highest tensile index for PFI mill refined BEK and Disc refined NBSK were approximately 113 ± 8.56 Nm/g and 97.77 ± 7.04 Nm/g respectively. The sheet density of most highly processed samples of PFI mill refined BEK and Disc refined NBSK showed 1012.45 ± 4.21 kg/m³ and 802.23 ± 28.05 kg/m³ respectively. It is worth noting that the specific energy consumption for the most heavily refined BEK and NBSK samples in PFI mill and Disc refiner were 17,417 kWh/t and 3346.3 kWh/t respectively, highlighting that Disc refining of NBSK is 5 times more energy efficient than PFI mill refining of BEK pulp. There is also a progressive increase in drainage time for both PFI mill refined BEK and Disc refined NBSK (Fig 1c).

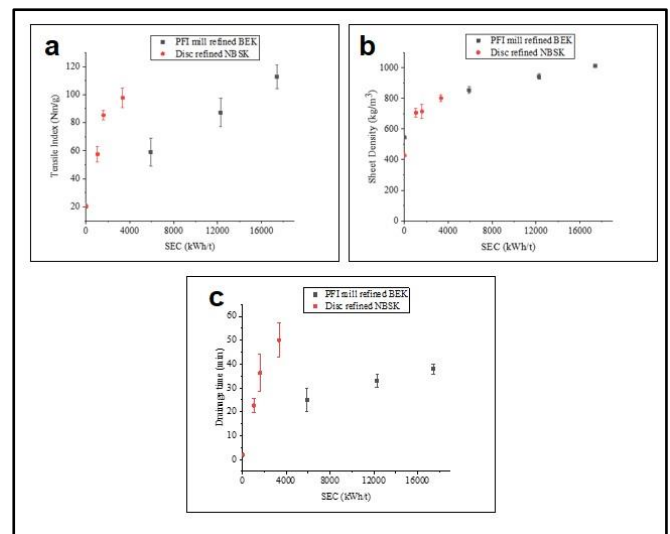


Fig 1: Mechanical property of nano cellulose sheets vs Specific energy consumption (PFI mill refined BEK and Disc refined) a) Tensile Index b) Sheet Density c) Drainage Time

FINES SCREENING BY BRECHT HOLL

Refining also produces small fibers with fines percentage reaching to 92.25 ± 1.06 % and 83.25 ± 4.59 % for NBSK 11 and BEK 50k respectively (Fig 2 a). Generation of fines

“ENERGY EFFICIENT NANOCELLULOSE SHEETS FOR PRODUCT APPLICATION”

during refining also leads to increase in dewatering time since fines have a high tendency to swell. An 75-80% fines content in NBSK & BEK refined pulp increases the drainage time by approximately 16-18 times when compared with drainage time taken for preparing unrefined NBSK and BEK sheets, respectively (Fig 2b). Refining also affects the geometry and number of fines content which directly increases the effective contact area for bonding enabling more uniform stress distribution, thus stronger sheets. The most heavily refined fibers BEK 50k (83.25% fines) and NBSK 11 (92.25% fines) enhances the sheet strength (tensile index) by approximately 5 times when compared with unrefined sheets (Fig 2c).

MIP PORE SIZE DISTRIBUTION AND POROSITY

The effect of refining on pore size distribution of nano cellulose sheet was studied by using mercury porosimetry (Fig 3). PFI mill refining for BEK and Disc refining for NBSK significantly reduced the pore size resulting in smaller diameter pore size distribution as shown by mercury intrusion volume peak (Fig 3a, 3b). The porosity is also plotted as a function of refining energy consumption, drainage time and fines. Most heavily processed BEK and NBSK sheets reduced porosity approximately by 50% and 60%, respectively as compared with unrefined sheets (Fig 4a, 4b, 4c). This comes at a cost of high drainage time of approximately 38 min and 50 min while preparing BEK and NBSK nanocellulose sheets respectively (Fig 4b). Refining causes an increase in number of fines which acts as fillers occupying the space of the pores, precisely where it is needed to significantly reduce the porosity of the porous unrefined sheets (Fig 4c).

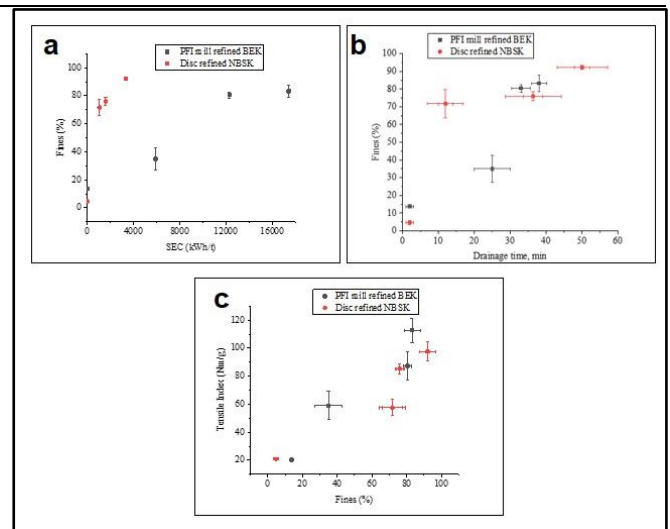


Fig 2 a) Fines (%) of nano cellulose (PFI mill refined BEK and Disc refined NBSK) as a function of a) Specific energy consumption) Drainage time vs. fines c) Tensile index vs fines

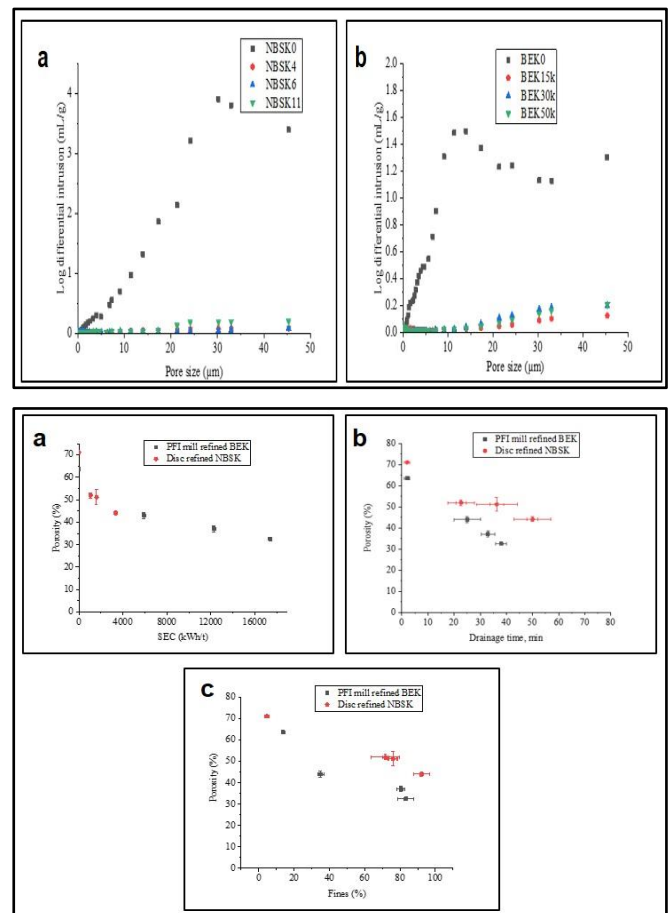


Fig 4 a) Porosity (%) vs SEC b) Porosity (%) vs Drainage time c) Porosity vs Fines (%)

SEM IMAGING AND DIAMETER DISTRIBUTION

Fiber diameter distribution of BEK and NBSK samples were determined from SEM images unrefined images of NBSK and BEK (Fig 1) were taken at appropriate magnification to show at least 80-100 individual fibres in total in the microscopy field. Fig 5a and 5b depicts the SEM images while fig 5c and 5d represent the diameter distribution of unrefined NBSK and BEK, respectively. Fig 6a and 6c shows the SEM images of moderately and highly disc refined NBSK while fig 6b and fig 6d represent that of moderately and highly lab refined BEK fibers. The diameter distribution of disc refined NBSK and lab refined BEK is compared in fig 6e and 6f, respectively. Industrial disc refining required 3346 kWh/t to reduce the diameter of NBSK fibres from 30-40 μm (NBSK0) to 40-60 nm (NBSK11)(Fig 5c and 6e). With expense of 17,417 kWh/t energy in PFI refining, BEK 50khas an order of 3 magnitude smaller fibre diameters and median diameter as compared with BEK 0k(Fig 5d and 6f). Fibre diameter reduction from micron (Fig 5a, 5b) to nano scale creates much compact and dense network which greatly reduces the accessible porosity (Fig 6a-6d). This clogging of pores through reduction of large fiber fraction (Fig 5a, 5b to Fig 6a, 6d) decreases the porosity of fibres.

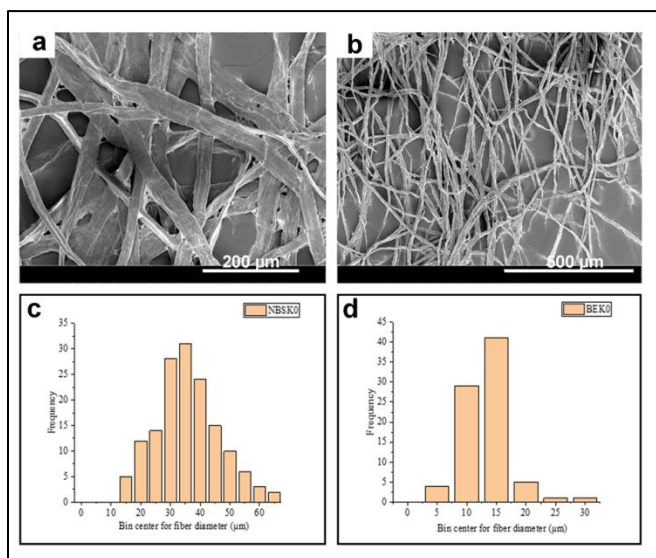
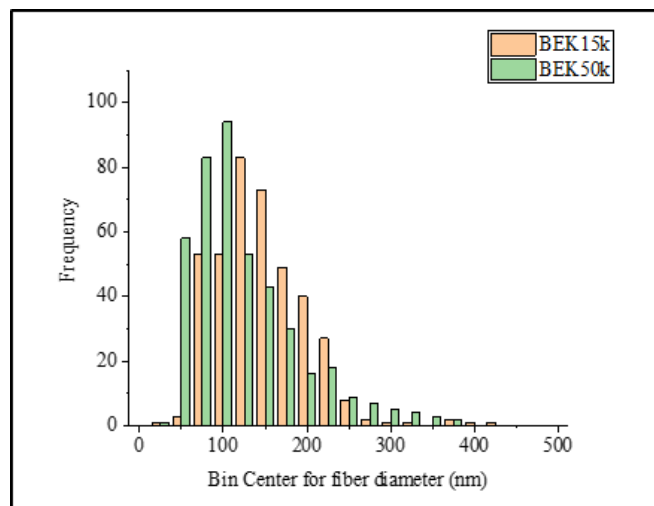
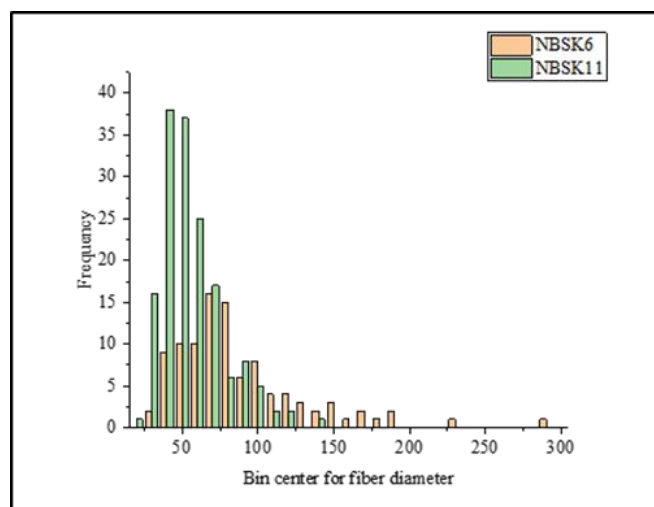
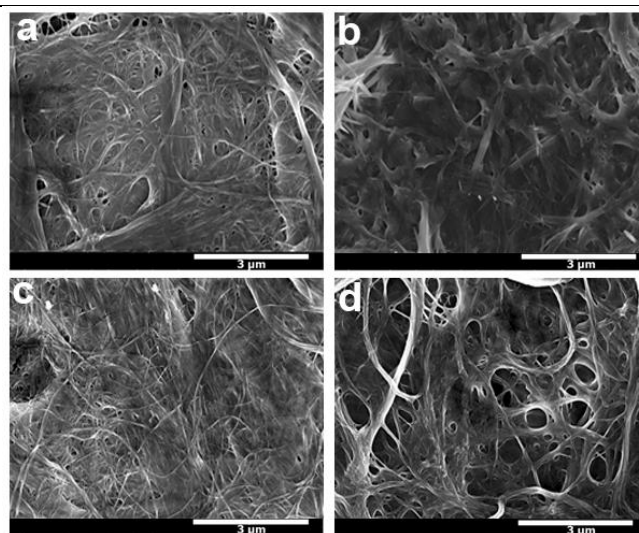


Fig 5 SEM images of a) unrefined NBSK0, b) unrefined BEK0, c) diameter distribution of unrefined NBSK0 and d) diameter distribution of unrefined BEK0

Fig 6 SEM images of a) unrefined NBSK0, b) unrefined BEK0, c) diameter distribution of unrefined NBSK0 and d) diameter distribution of unrefined BEK0

WATER VAPOR PERMEABILITY

The water vapour permeability was measured in triplicate for all samples. The results are compared in Fig 7a as a function of refining energy consumption. There is approximately ten times reduction in water vapour permeability with refining as compared with unrefined sheets for both NBSK and BEK sheets respectively. However, the rate of decrease reaches a threshold and there is not much improvement after certain level of refining. Thickness is one of the major parameters which gets lowered with refining thus improving the barrier property of the nano cellulose sheet (Fig 7b). Sheet density also seems to be directly correlated with barrier properties. An approximate two times sheet densification due to progressive refining has decreased water vapour permeability by ten times for both BEK and NBSK sheets (Fig 7c). Fines content which seems to be improving bonding between the fibers also seems to improve water vapour permeability. At around 80% of fines approximate WVP values found was 3×10^{-11} g/Pa.s.m for both BEK and NBSK sheets (Fig 7d).

AIR PERMEANCE AND OXYGEN PERMEABILITY

The air permeance of highly porous NBSK0 sheet was not detected however, BEK0 unrefined sheet had an air permeance of $45.52 \pm 4.14 \mu\text{m}^2/\text{Pa.s}$. The oxygen permeability of refined nano cellulose sheet decreased by 99.30% and 95.75% for BEK and NBSK respectively (Fig 8). The oxygen permeability of refined nano cellulose sheet was plotted as a function of specific energy consumption and declining trend was observed to reach plateau (Fig 8a). Fig 8b, 8c and 8d also show the effect of thickness, porosity and fines on the permeability of oxygen molecule towards nano cellulose sheet. A 24.42% and 99.31% reduction in porosity gave an oxygen permeability of 0.53 ± 0.09 and $0.76 \pm 0.03 \text{cc} \cdot \mu\text{m}^2/\text{m}^2 \cdot \text{day} \cdot \text{kPa}$ for BEK and NBSK nano cellulose sheets respectively (Fig 8c). An increase in fines from 35% to 80% leads to lowering of oxygen permeability of refined NBSK and BEK sheets to approximately $1 \text{cm}^3 \cdot \mu\text{m}^2/\text{m}^2 \cdot \text{day} \cdot \text{kPa}$ (Fig 8d).

SURFACE ROUGHNESS

The aerial and root mean square roughness parameters of nano cellulose sheets were evaluated in triplicate from optical pro filometer images. The surface roughness results from coarseness, irregularities on nano cellulose which evaluates vertical deviation from actual surface through parameters like aerial surface roughness (S_a) and root mean square surface roughness (S_q). While S_a is more statistically stable however S_q is more authentic as it provides information about peaks and valleys on nano cellulose surface (Shanmugam et al. 2020). Fig 9a and Fig 9b (dotted line) shows that to reach approximately $1 \mu\text{m}$ and $1.5 \mu\text{m}$ S_q roughness; it requires 3346 kWh/t and 17417 kWh/t of energy for Disc refined NBSK and PFI mill refined BEK respectively. An 77.05% and 52.8% enhancement in smoothness of nano cellulose sheets can be observed from fig 9a, 9b. The trends in fig 9c and 9d suggest that there is strong relationship between refining level and surface roughness, from which we may be able to extrapolate the degree of refining required to produce acceptable nano cellulose smoothness for printing applications. The rough side roughness (S_a , S_q) is also measured and it is also having similar trend with both PFI and Disc refining levels (Fig S2). The optical pro filometer images of rough and smooth side of NBSK and BEK is also shown at various levels of refining (Fig S3, Fig S4). Fig 10 highlights and support our findings as fines percentage goes up with refining level there is approximately 572% and 1136% enhancement in transmittance in the visible region (400nm-700nm) for NBSK11 & BEK50k respectively, as compared with unrefined sheets (Fig 10a, b). This supports our observation with SEM images and fiber diameter distribution that with refining there is a continuous production of smaller diameter fiber (nm sized range) below the wavelength of visible light (400-700nm), that is the potential reason it is showing higher transmittance as opposed unrefined fibers. Unrefined fibers are in micron scale and usually scatter some or all visible incident light on them, which is indicative from the plots (Fig 10a, b).

“ENERGY EFFICIENT NANOCELLULOSE SHEETS FOR PRODUCT APPLICATION”

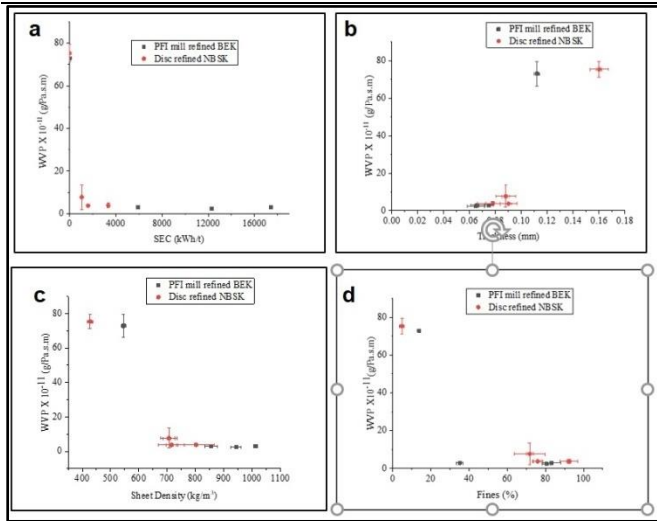


Fig 7: Water Vapor permeability properties of nanocellulose sheets a) WVP vs SEC b) WVP vs thickness, c) WVP vs sheet density and d) WVP vs fines (%)

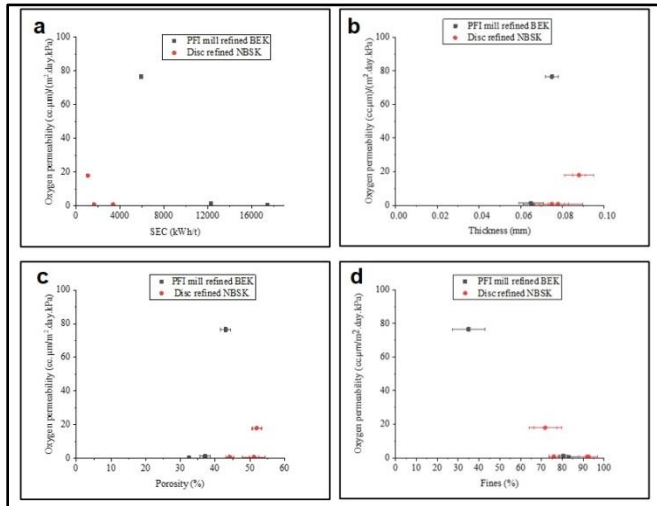


Fig 8: Oxygen permeability of refined nanocellulose sheets a) Oxygen permeability vs SEC, b) Oxygen permeability vs

thickness, c) Oxygen permeability vs porosity and d) Oxygen permeability vs Fines%

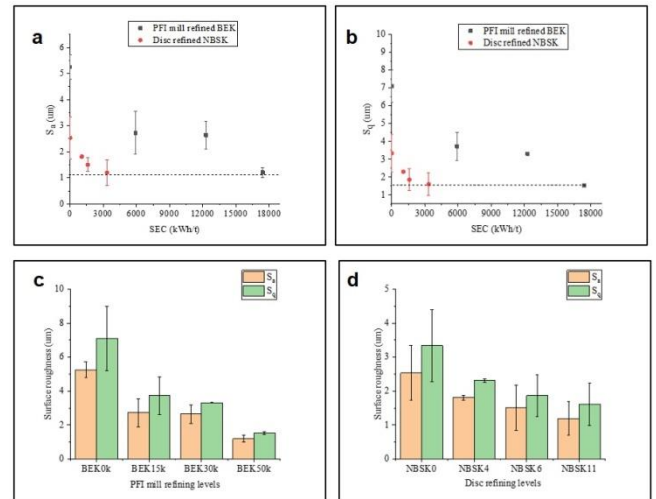


Fig 9: Smooth side Surface roughness as a function of SEC a) Sa vs SEC b) Sq vs SEC and refining level c) PFI mill refining and d) Disc refining

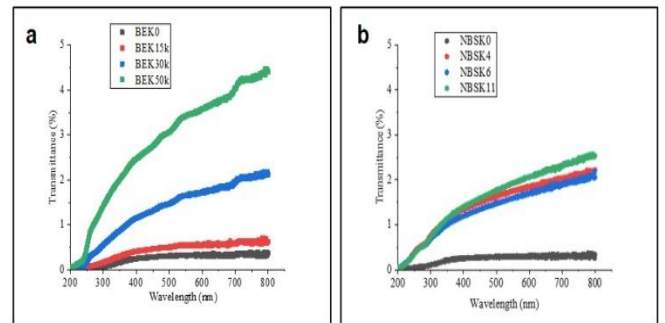


Fig 10: Transmittance of nano cellulose sheet at various levels of refining

“ENERGY EFFICIENT NANOCELLULOSE SHEETS FOR PRODUCT APPLICATION”

Table 1: Literature comparison of **oxygen permeability** of common packaging materials with synthetic films and polyme

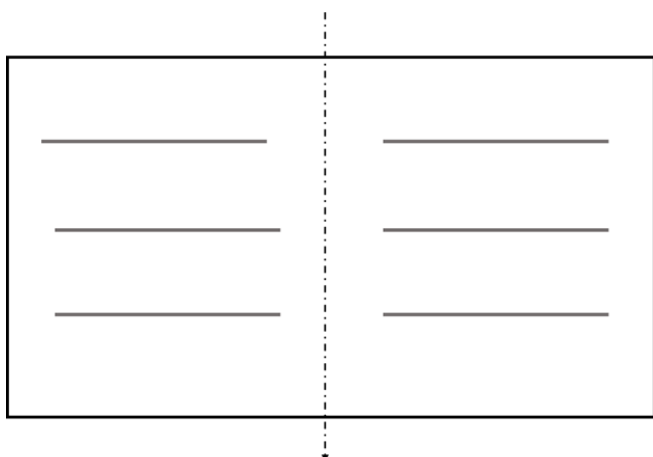
Material	Oxygen permeability (cc μm)/ (m ² daykPa)	Temperature & Relative Humidity (%)	Reference
Nanocellulose film	0.6	65%, RH 23°C	(Österberg et al. 2013)
Nanocellulose (carboxymethylated)	0.85	50% RH, 23°C	(Aulin, Gällstedt, and Lindström 2010)
Polyethylene (PE)	500-2000	50% RH, 23°C	(Lange and Wyser 2003)
Polyvinylidene chloride (PVDC)	0.1-3	50% RH, 23°C	(Lange and Wyser 2003)
Ethylene vinyl alcohol (EVOH)	0.01-0.1	50% RH, 23°C	(Lange and Wyser 2003)
Polyethylene terephthalate (PET)	10-50	50% RH, 23°C	(Lange and Wyser 2003)
Low density polyethylene (LDPE)	1900	50% RH, 23°C	(Aulin, Gällstedt, and Lindström 2010)
Experimental BEK& NBSK Nanocellulose sheet			
BEK15k	76.55	50% RH, 23°C	Present study
BEK30k	1.244	50% RH, 23°C	
BEK50k	0.533	50% RH, 23°C	
NBSK4	17.944	50% RH, 23°C	
NBSK6	0.763	50% RH, 23°C	
NBSK11	0.762	50% RH, 23°C	

“ENERGY EFFICIENT NANOCELLULOSE SHEETS FOR PRODUCT APPLICATION”

Table 2: Literature comparison of **water vapor permeability** of common packaging materials with synthetic films and polymers

Material	Water vapour permeability (g/m ² day)	Average film thickness (µm)	Water Vapour Permeability (g/m.s.Pa)	Testing conditions & Reference
Nano cellulose	234	42	8.12*10 ⁻¹¹	(Rodionova et al. 2011), 50% RH
Acetylated Nano cellulose	167	46	6.35*10 ⁻¹¹	(Rodionova et al. 2011), 50% RH
Polyethylene (PE)	16.8	18.3	1.00*10 ⁻¹²	(Steven and Hotchkiss 2002), 100% RH
Polyvinylidene chloride (PVDC)	3.07	12.7	1.27*10 ⁻¹³	(Steven and Hotchkiss 2002), 100% RH
Ethylene vinyl alcohol (EVOH)	22-124	25	1.07 *10 ⁻¹² - 6.032*10 ⁻¹²	(Bhunias et al. 2013), 38°C 90% RH
Polyethylene terephthalate (PET)	16-23	25	7.78 *10 ⁻¹³ - 1.12*10 ⁻¹²	(Bhunias et al. 2013), 38°C 90% RH
Low density polyethylene (LDPE)	18	25	8.75*10 ⁻¹³	38°C, 90% RH*
Experimental BEK & NBSK Nano cellulose sheet				
BEK0k	789.410	112	72.93*10 ⁻¹¹	Present study, 50% RH, 23°C
BEK15k	47.314	72	2.91*10 ⁻¹¹	
BEK30k	44.783	65	2.39*10 ⁻¹¹	
BEK50k	55.410	66	3*10 ⁻¹¹	
NBSK0	571.816	160	75.3*10 ⁻¹¹	
NBSK4	58.826	88	7.7*10 ⁻¹¹	
NBSK6	50.350	86	3.75*10 ⁻¹¹	
NBSK11	54.651	75	3.86*10 ⁻¹¹	

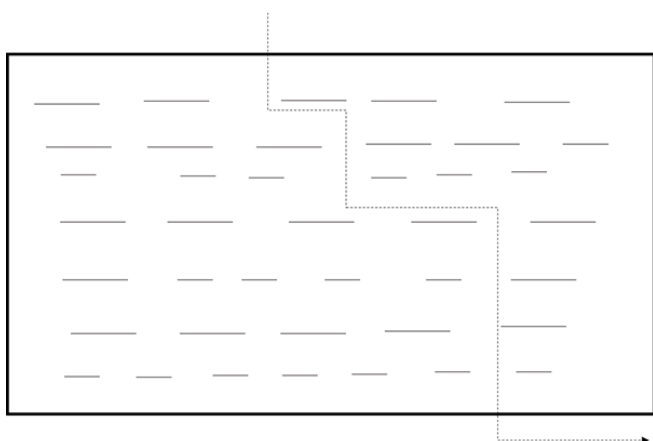
a) Permeating molecule (oxygen, water vapour)



**Unrefined
Cellulose sheet**

- Porous
- Thicker
- Micron scale fiber diameter
- Poor barrier properties

b) Permeating molecule (oxygen, water vapour)



**Unrefined
Cellulose sheet**

- Porous
- Thicker
- Micron scale fiber diameter
- Poor barrier properties

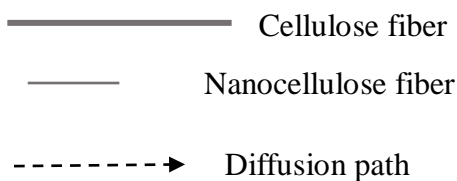


Fig 11: Schematic representation of increased tortuosity with nanocellulose sheets a) Unrefined cellulose sheets, b) Refined nanocellulose sheets

DISCUSSION

The effect of refining on nano cellulose fibers and sheets was tested at range of refining conditions for both disc refined softwood (NBSK) and lab refined hardwood samples (BEK). A constant increase in mechanical energy consumption in refining leads to enhancement in both oxygen permeability and water vapor permeability, however there is a plateau beyond which there is no further improvement (Table 1& Table 2).

There is an improvement in mechanical sheet properties like sheet density, tensile index and also an increase in drainage time with progressive refining. This is mainly because during PFI mill and Disc refining there is both external and internal fibrillation caused by the compression effects in refining (Nugroho 2012). Internal fibrillation (peeling of primary and secondary cell wall) causes breakage of inner bonds making the fiber more flexible impacting the bonding ability which is a key factor to enhance sheet density and tensile strength (Fernando et al. 2011). This results in increase in fibril area and dense network structure decreasing pore size and porosity of sheets. Refining also exposes the surface functional groups which makes hydrogen bonding better making molecules difficult to pass through which is excellent for barrier properties (Nair et al. 2014). The 3 order of magnitude reduction in fiber diameter that occurs when cellulose fibers are broken down into nano fiber allows for production of nano cellulose which have high strength, high specific surface area, and good barrier properties (Osong, Norgren, and Engstrand 2016; Siró and Plackett 2010). Further with progressive refining decrease in median nano cellulose fiber diameters from 135 nm to 71 nm for BEK and 78 nm to 45.2 nm for NBSK (Fig 6) was observed which would result in significantly larger surface area available for bonding. Refining is also associated with increase in fines production (González et al. 2013; Zeng et al. 2012). Fines are defined as particle which passes through a 76 µm screen have much larger specific surface area, also they fill interfiber space during sheet dewatering, increases fiber-fiber interaction, and improves bonds strength and

sheet solidification (Seth 2003). Fines also increases drainage time due to decrease in sheet porosity.

The diffusion process of the molecules between nano cellulose sheets happens in three steps: adsorption of molecule on to the surface, followed by intermolecular diffusion and desorption from membrane surface (Nair et al. 2014). Refining decreases porosity of nano cellulose due to substantial increase of narrow pores in the sheets. Thus, a dense non-porous film of nano cellulose may present a high tortuosity for diffusion of gas molecules (Fig 11). Thus, refining has a positive impact on WVP and air permeability due to the formation of small agglomerates. Also, it enhances the smoothness of nano cellulose sheet which can have a potential impact in controlling their application in printed electronics(Shanmugam et al. 2020).

The potential of refining on NC film as packaging material can be evaluated through comparing with numerous synthetic and other cellulose polymers. The WVTR of approximately 33g/m², 42 µm thickness pure nano cellulose sheet is 234g/m².day which is somewhat above WVPs of plastic packaging materials. For example, Polyethylene (PE), Polyvinylidene chloride (PVDC), EVOH are 16.8g/m².day, 3.07g/m².day, 22-124 g/m².day respectively (Table 1). However, this difference can be overcome by using refined 60 gsm nanocellulose sheet, which then attains WVTR around 44.78-58.83 g/m² day. The water vapor permeability (WVP) values of refine nanocellulose sheet which are normalised by thickness and pressure term are also very close with that of plastic packaging material. This demonstrates the applicability of refining products and suitability of fiber refining as a suitable and promising alternative for synthetic packaging.

Nano cellulose related films has the potential to increase shelf life of food by limiting the permeation of oxygen (Shimizu, Saito, and Isogai 2016; Aulin, Gällstedt, and Lindström 2010). The oxygen permeability obtained after refining are competitively with petroleum based and polymeric packaging material (Table 1). Moreover, refining process used here is an eco-friendly, sustainable scalable process which can be successfully demonstrated as an alternative to

synthetic polymers. The strength of nano cellulose films is also impacted by the effects of refining where 369.15% and 452.55% enhancement in tensile index was observed for NBSK and BEK nano cellulose sheets respectively as compared with unrefined BEK and NBSK (Fig 1a). The SEM of nano cellulose films (moderately and heavily refined) and transmittance result shows that fiber diameter getting smaller with more production of fines. This is critical as network of pores in nano cellulose is controlling parameter in barrier performance. The extent to which tortuosity can account for reductions in permeability through refining is a topic that merits further research attention. The barrier properties for oxygen are excellent for nano cellulose, however they have poor water vapor barrier properties due to high affinity between water and nano cellulose sheets(Nair et al. 2014).

While polymers and plastics, such as polyethylene, LDPE are low cost, durable and can be easily fabricated however they are non-biodegradable and non-renewable which poses a serious threat to the ecosystem. There is a growing need to tackle the environmental problems which is due to overconsumption of plastics. The global production of plastics has increased twentyfold and has reached 322 million tonnes in 2015 which gives accumulates globally approximately 400 million tonnes of CO₂ a year (Strategy 2018). This is coupled with substantial plastic waste disposal problem generating plastic pollution in oceans. To reduce over reliance on plastics and to protect the environment, the European commission has introduced and implemented new rules to reduce amount of single-use plastics in areas such as packaging which will raise the cost of plastic packaging (Watkins and Schweitzer 2018). This has led to an upsurge of interest and research related with nanocellulose composite materials for packaging(Ferrer, Pal, and Hubbe 2017; Hubbe et al. 2017). This has led to the development of nanocellulose as barrier material to meet the demand of packaging barrier materials in a sustainable manner (Kim et al. 2015). The mechanical energy consumption during refining thus can be optimised to

produce smoother, less porous, dense and highly transparent nano cellulose sheets over traditional unrefined cellulosic papers.

Disc refining consumes five times less refining energy in producing nano cellulose with softwood NBSK pulps as compared with PFI mill refining of hardwood BEK pulp. The barrier properties of nano cellulose sheets reached a plateau at 12,292 kWh/t in PFI mill and 1599.9 kWh/t in Disc refining, which further sheds light that very high energy consumption is not necessary to produce nano cellulose with good barrier properties. While production of nano cellulose has its own limitation with higher land use and significant water consumption it is crucial that the energy to cost performance criteria for nano cellulose be properly addressed to compete with economies of packaging raw materials. The lab facilities are not sustainable when compared with industrial scale nanocellulose production (Li et al. 2013; Piccinno et al. 2018). Assuming most of the energy consumption of nanocellulose production happens during refining, disc refining is approximately ten times more energy efficient than conventional packaging films (Mohamed et al. 2014; Impee 2005). Thus, considering energy consumption over packaging materials, nanocellulose produced at industrial scale could be more sustainable and it is certainly worthy in wide range of packaging applications.

CONCLUSION

Refining or beating is a mechanical treatment of the pulp fibers which improves the final properties of nanocellulose sheets. The effect of mechanical refining is attributed to change of mechanical and geometrical properties of fibers and fiber bonds which is mainly because of internal fibrillation of cell wall structure of cellulose. The increase conformability and flexibility due to refining leads to larger bonded areas, strong bond between fibers which enhances tensile index, sheet density. Disc refining of NBSK pulp was 5 times more energy efficient than PFI mill refining of BEK. At 17,417 kWh/t SEC PFI mill refined BEK achieved a tensile index of approximately 112 Nm/g however it took

only 3346.3 kWh/t SEC to achieve similar result for Disc refined NBSK. Fines formation which increases the drainage time for nano cellulose sheet formation enhanced the barrier property of the nano cellulose sheets both in terms of oxygen and water vapor permeability. Greater degree of fibrillation decreases the mean fiber diameter of both NBSK and BEK pulp by three orders of magnitude. This positively influences the porosity and fines formation. Thus, due to refining there is a tortuosity of the diffusion path by the permeating molecule which improves the barrier property of refined nano cellulose sheets. The water vapor and oxygen permeability values are comparable with that of polymers and thus refining of cellulose can be a huge potential for upcoming packaging industry. There is also a plateau observed for barrier properties, fines formation which means a trade-off can be achieved between energy consumption and product application for sustainable production of nano cellulose.

REFERENCES

1. Abdollahi, Mehdi, Mehdi Alboofetileh, Rabi Behrooz, Masoud Rezaei, and Reza Miraki. 2013. 'Reducing water sensitivity of alginate bio-nanocomposite film using cellulose nanoparticles', *International journal of biological macromolecules*, 54: 166-73.
2. Agate, Sachin, Michael Joyce, Lucian Lucia, and Lokendra Pal. 2018. 'Cellulose and nanocellulose-based flexible-hybrid printed electronics and conductive composites—a review', *Carbohydrate polymers*, 198: 249-60.
3. Ahmadzadeh, Safoura, Ali Nasirpour, Javad Keramat, Nasser Hamdami, Tayebbeh Behzad, and Stephane Desobry. 2015. 'Nanoporous cellulose nanocomposite foams as high insulated food packaging materials', *Colloids and Surfaces A: Physicochemical and Engineering Aspects*, 468: 201-10.
4. Alves, JS, KC Dos Reis, EGT Menezes, FV Pereira, and J Pereira. 2015. 'Effect of cellulose nanocrystals and gelatin in corn starch plasticized films', *Carbohydrate polymers*, 115: 215-22.
5. Ang, Shaun, Victoria Haritos, and Warren Batchelor. 2019. 'Effect of refining and homogenization on nanocellulose fiber development, sheet strength and energy consumption', *Cellulose*, 26: 4767-86.
6. ASTM, F. 1927. "07. Standard Test Method for Determination of Oxygen Gas Transmission Rate, Permeability and Permeance at Controlled Relative Humidity Through Barrier Materials Using a Coulometric Detector. American National Standards Institute. Aug. 2007." In.
7. Aulin, Christian, Mikael Gällstedt, and Tom Lindström. 2010. 'Oxygen and oil barrier properties of microfibrillated cellulose films and coatings', *Cellulose*, 17: 559-74.
8. Aulin, Christian, German Salazar-Alvarez, and Tom Lindström. 2012. 'High strength, flexible and transparent nanofibrillated cellulose–nanoclay biohybrid films with tunable oxygen and water vapor permeability', *Nanoscale*, 4: 6622-28.
9. Bhunia, Kanishka, Shyam S Sablani, Juming Tang, and Barbara Rasco. 2013. 'Migration of chemical compounds from packaging polymers during microwave, conventional heat treatment, and storage', *Comprehensive Reviews in Food Science and Food Safety*, 12: 523-45.
10. El Miri, Nassima, Karima Abdelouahdi, Abdellatif Barakat, Mohamed Zahouily, Aziz Fihri, Abderrahim Solhy, and Mounir El Achaby. 2015. 'Bio-nanocomposite films reinforced with cellulose nanocrystals: Rheology of film-forming solutions, transparency, water vapor barrier and tensile properties of films', *Carbohydrate polymers*, 129: 156-67.
11. Fernando, Dinesh, Dino Muhić, Per Engstrand, and Geoffrey Daniel. 2011. 'Fundamental understanding of pulp property development under different thermomechanical pulp refining

- conditions as observed by a new Simons’ staining method and SEM observation of the ultrastructure of fibre surfaces', *Holzforschung*, 65: 777-786.
12. Ferrer, Ana, Lokendra Pal, and Martin Hubbe. 2017. 'Nanocellulose in packaging: Advances in barrier layer technologies', *Industrial Crops and Products*, 95: 574-82.
 13. Fukuzumi, Hayaka, Tsuguyuki Saito, Tadahisa Iwata, Yoshiaki Kumamoto, and Akira Isogai. 2009. 'Transparent and high gas barrier films of cellulose nanofibers prepared by TEMPO-mediated oxidation', *Biomacromolecules*, 10: 162-65.
 14. Garusinghe, Uthpala M, Swambabu Varanasi, Vikram S Raghuvanshi, Gil Garnier, and Warren Batchelor. 2018. 'Nanocellulose-montmorillonite composites of low water vapour permeability', *Colloids and Surfaces A: Physicochemical and Engineering Aspects*, 540: 233-41.
 15. Giesche, Herbert. 2006. 'Mercury porosimetry: a general (practical) overview', *Particle & particle systems characterization*, 23: 9-19.
 16. González, I, F Vilaseca, M Alcalá, MA Pèlach, S Boufi, and P Mutjé. 2013. 'Effect of the combination of biobeating and NFC on the physico-mechanical properties of paper', *Cellulose*, 20: 1425-35.
 17. Ho, Thao TT, Tanja Zimmermann, Steffen Ohr, and Walter R Caseri. 2012. 'Composites of cationic nanofibrillated cellulose and layered silicates: water vapor barrier and mechanical properties', *ACS applied materials & interfaces*, 4: 4832-40.
 18. Hoeng, Fanny, Aurore Denneulin, and Julien Bras. 2016. 'Use of nanocellulose in printed electronics: a review', *Nanoscale*, 8: 13131-54.
 19. Honorato, Camila, Vinay Kumar, Jun Liu, Hanna Koivula, Chunlin Xu, and Martti Toivakka. 2015. 'Transparent nanocellulose-pigment composite films', *Journal of materials science*, 50: 7343-52.
 20. Hubbe, Martin A, Ana Ferrer, Preeti Tyagi, Yuanyuan Yin, Carlos Salas, Lokendra Pal, and Orlando J Rojas. 2017. 'Nanocellulose in thin films, coatings, and plies for packaging applications: A review', *BioResources*, 12: 2143-233.
 21. Hyll, Kari. 2015. 'Size and shape characterization of fines and fillers-a review', *Nordic Pulp & Paper Research Journal*, 30: 466-87.
 22. Impee, P. 2005. 'Recycling of plastics', *The impee project university of cambridge*.
 23. Isogai, Akira. 2013. 'Wood nanocelluloses: fundamentals and applications as new bio-based nanomaterials', *Journal of wood science*, 59: 449-59.
 24. Johansson, Caisa, Julien Bras, Iñaki Mondragon, Petronela Nechita, David Plackett, Peter Simon, Diana Gregor Svetec, Sanna Virtanen, Marco Giacinti Baschetti, and Chris Breen. 2012. 'Renewable fibers and bio-based materials for packaging applications—a review of recent developments', *BioResources*, 7: 2506-52.
 25. Kim, Joo-Hyung, Bong Sup Shim, Heung Soo Kim, Young-Jun Lee, Seung-Ki Min, Daseul Jang, Zafar Abas, and Jaehwan Kim. 2015. 'Review of nanocellulose for sustainable future materials', *International Journal of Precision Engineering and Manufacturing-Green Technology*, 2: 197-213.
 26. Kumar, Saurabh. 2012. 'Deinking pulp fractionation: characterization and separation of fines by screening'.
 27. Kuswandi, B. 2017. 'Environmental friendly food nano-packaging', *Environmental Chemistry Letters*, 15: 205-21.
 28. Lange, J, and Yves Wyser. 2003. 'Recent innovations in barrier technologies for plastic packaging—a review', *Packaging Technology and Science: An International Journal*, 16: 149-58.
 29. Lavoine, Nathalie, Isabelle Desloges, Alain Dufresne, and Julien Bras. 2012. 'Microfibrillated cellulose—Its barrier properties and applications in

- cellulosic materials: A review', *Carbohydrate polymers*, 90: 735-64.
30. Li, Fei, Erika Mascheroni, and Luciano Piergiovanni. 2015. 'The potential of nanocellulose in the packaging field: a review', *Packaging Technology and Science*, 28: 475-508.
31. Li, Qingqing, Sean McGinnis, Cutter Sydnor, Anthony Wong, and Scott Rennecker. 2013. 'Nanocellulose life cycle assessment', *ACS Sustainable Chemistry & Engineering*, 1: 919-28.
32. Mohamed, Radin Maya Saphira Radin, Gazala Sanusi Misbah, Anwaruddin Ahmed Wurochekke, and Amir Hashim bin Mohd Kassim. 2014. 'Energy recovery from polyethylene terephthalate (PET) recycling process', *GSTF Journal of Engineering Technology (JET)*, 2: 1-6
33. Nair, Sandeep S, JY Zhu, Yulin Deng, and Arthur J Ragauskas. 2014. 'High performance green barriers based on nanocellulose', *Sustainable Chemical Processes*, 2: 23.
34. Nakagaito, Antonio Norio, and Hiroyuki Yano. 2005. 'Novel high-strength biocomposites based on microfibrillated cellulose having nano-order-unit web-like network structure', *Applied Physics A*, 80: 155-59.
35. Nugroho, Dimas Dwi Prasetyo. 2012. 'Low consistency refining of mixtures of softwood & hardwood bleached kraft pulp: effects of refining power', *Asian Institute of Technology*.
36. Okada, Akane, and Arimitsu Usuki. 2006. 'Twenty years of polymer-clay nanocomposites', *Macromolecular materials and Engineering*, 291: 1449-76.
37. Osong, Sinke H, Sven Norgren, and Per Engstrand. 2016. 'Processing of wood-based microfibrillated cellulose and nanofibrillated cellulose, and applications relating to papermaking: a review', *Cellulose*, 23: 93-123.
38. Österberg, Monika, Jari Vartiainen, Jessica Lucenius, Ulla Hippi, Jukka Seppälä, Ritva Serimaa, and Janne Laine. 2013. 'A fast method to produce strong NFC films as a platform for barrier and functional materials', *ACS applied materials & interfaces*, 5: 4640-47.
39. Paralikar, Shweta A, John Simonsen, and John Lombardi. 2008. 'Poly (vinyl alcohol)/cellulose nanocrystal barrier membranes', *Journal of Membrane Science*, 320: 248-58.
40. Piccinno, Fabiano, Roland Hischer, Stefan Seeger, and Claudia Som. 2018. 'Predicting the environmental impact of a future nanocellulose production at industrial scale: Application of the life cycle assessment scale-up framework', *Journal of Cleaner Production*, 174: 283-95
41. Rhim, Jong-Whan, and Perry KW Ng. 2007. 'Natural biopolymer-based nanocomposite films for packaging applications', *Critical reviews in food science and nutrition*, 47: 411-33.
42. Rodionova, Galina, Marianne Lenes, Øyvind Eriksen, and Øyvind Gregersen. 2011. 'Surface chemical modification of microfibrillated cellulose: improvement of barrier properties for packaging applications', *Cellulose*, 18: 127-34.
43. Sehaqui, Houssine, Andong Liu, Qi Zhou, and Lars A Berglund. 2010. 'Fast preparation procedure for large, flat cellulose and cellulose/inorganic nanopaper structures', *Biomacromolecules*, 11: 2195-98.
44. Sehaqui, Houssine, Seira Morimune, Takashi Nishino, and Lars A Berglund. 2012. 'Stretchable and strong cellulose nanopaper structures based on polymer-coated nanofiber networks: An alternative to nonwoven porous membranes from electrospinning', *Biomacromolecules*, 13: 3661-67.
45. Seth, RS. 2003. 'measurement and significance of fines', *Pulp & Paper Canada*.
46. Shanmugam, Kirubanandan, Humayun Nadeem, Christine Browne, Gil Garnier, and Warren Batchelor. 2020. 'Engineering surface roughness of nanocellulose film via spraying to produce smooth

- substrates', *Colloids and Surfaces A: Physicochemical and Engineering Aspects*, 589: 124396
47. Sharma, Sudhir, Xiaodan Zhang, Sandeep S Nair, Arthur Ragauskas, Junyong Zhu, and Yulin Deng. 2014. 'Thermally enhanced high performance cellulose nano fibril barrier membranes', *RSC Advances*, 4: 45136-42.
48. Shimizu, Michiko, Tsuguyuki Saito, and Akira Isogai. 2016. 'Water-resistant and high oxygen-barrier nanocellulose films with interfibrillar cross-linkages formed through multivalent metal ions', *Journal of Membrane Science*, 500: 1-7.
49. Silvério, Hudson Alves, Wilson Pires Flauzino Neto, and Daniel Pasquini. 2013. 'Effect of incorporating cellulose nanocrystals from corncob on the tensile, thermal and barrier properties of poly (vinyl alcohol) nanocomposites', *Journal of Nanomaterials*, 2013.
50. Sim, Kyujeong, and Hye Jung Youn. 2016. 'Preparation of porous sheets with high mechanical strength by the addition of cellulose nanofibrils', *Cellulose*, 23: 1383-92.
51. Siró, István, and David Plackett. 2010. 'Microfibrillated cellulose and new nanocomposite materials: a review', *Cellulose*, 17: 459-94.
52. Stankovská, Monika, Juraj Gigac, Mária Fišerová, and Elena Opálená. 2019. 'RELATIONSHIP BETWEEN STRUCTURAL PARAMETERS AND WATER ABSORPTION OF BLEACHED SOFTWOOD AND HARDWOOD KRAFT PULPS', *WOOD RESEARCH*, 64: 261-72.
53. Steven, Matthew D, and Joseph H Hotchkiss. 2002. 'Comparison of flat film to total package water vapour transmission rates for several commercial food wraps', *Packaging Technology and Science: An International Journal*, 15: 17-27.
54. Strategy, Plastic. 2018. 'A European strategy for plastics in a circular economy', *Communication from the Commission to the European Parliament, the Council, the European Economic and Social Committee and the Committee of the Regions. Brussels.*
55. Thao Ho, Thi Thu, Tanja Zimmermann, Walter Remo Caseri, and Paul Smith. 2013. 'Liquid ammonia treatment of (cationic) nanofibrillated cellulose/vermiculite composites', *Journal of Polymer Science Part B: Polymer Physics*, 51: 638-48.
56. Tharanathan, RN. 2003. 'Biodegradable films and composite coatings: past, present and future', *Trends in food science & technology*, 14: 71-78.
57. Tingaut, Philippe, Tanja Zimmermann, and Francisco Lopez-Suevos. 2010. 'Synthesis and characterization of bionanocomposites with tunable properties from poly (lactic acid) and acetylated microfibrillated cellulose', *Biomacromolecules*, 11: 454-64.
58. Varanasi, Swambabu, and Warren J Batchelor. 2013. 'Rapid preparation of cellulose nanofibre sheet', *Cellulose*, 20: 211-15.
59. Watkins, Emma, and Jean-Pierre Schweitzer. 2018. 'Moving towards a circular economy for plastics in the EU by 2030.' in, *Think 2030. Brussels: Institute for European Environmental Policy (IEEP).*
60. Youssef, Ahmed M, Magda Ali El-Samahy, and Mona H Abdel Rehim. 2012. 'Preparation of conductive paper composites based on natural cellulosic fibers for packaging applications', *Carbohydrate polymers*, 89: 1027-32.
61. Zeng, Xiling, Shiyu Fu, Elias Retulainen, and Sabine Heinemann. 2012. 'Fibre deformations induced by different mechanical treatments and their effect on zero-span strength', *Nordic Pulp & Paper Research Journal*, 27: 335-42.
62. Zhang, Liyuan, Warren Batchelor, Swambabu Varanasi, Takuya Tsuzuki, and Xungai Wang. 2012. 'Effect of cellulose nanofiber dimensions on sheet forming through filtration', *Cellulose*, 19: 561-74.

SUPPLEMENTARY INFORMATION FOR ENERGY EFFICIENT NANOCELLULOSE SHEET FOR PACKAGING APPLICATION

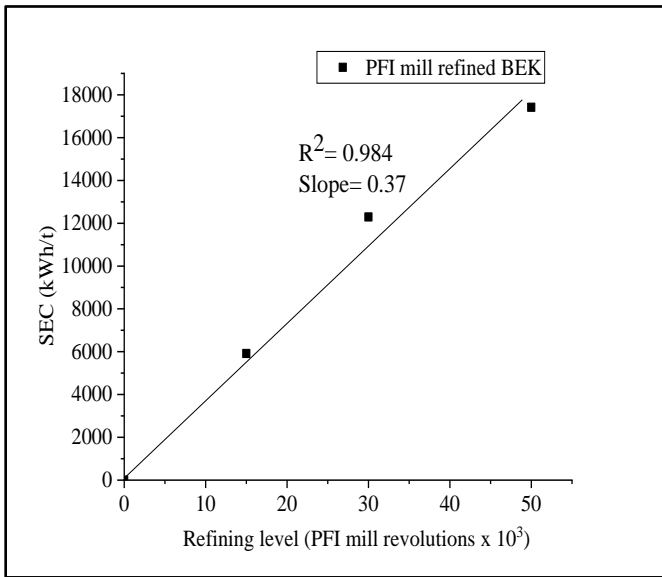


Figure S1a: Specific energy consumption (SEC) for PFI mill refining of BEK pulp versus refining level in revolutions

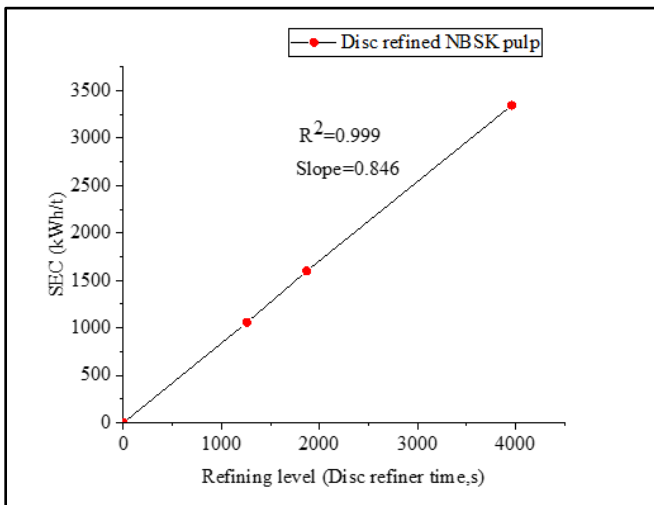


Figure S1b: Specific energy consumption (SEC) for industrial disc refining of NBSK pulp versus refining level in seconds.

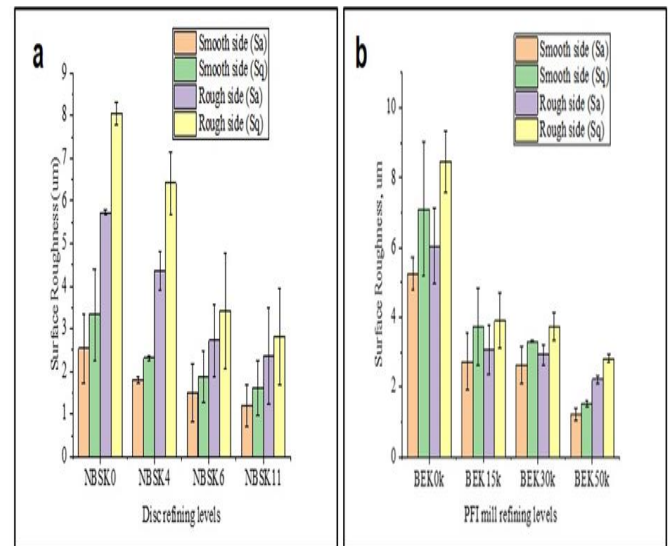
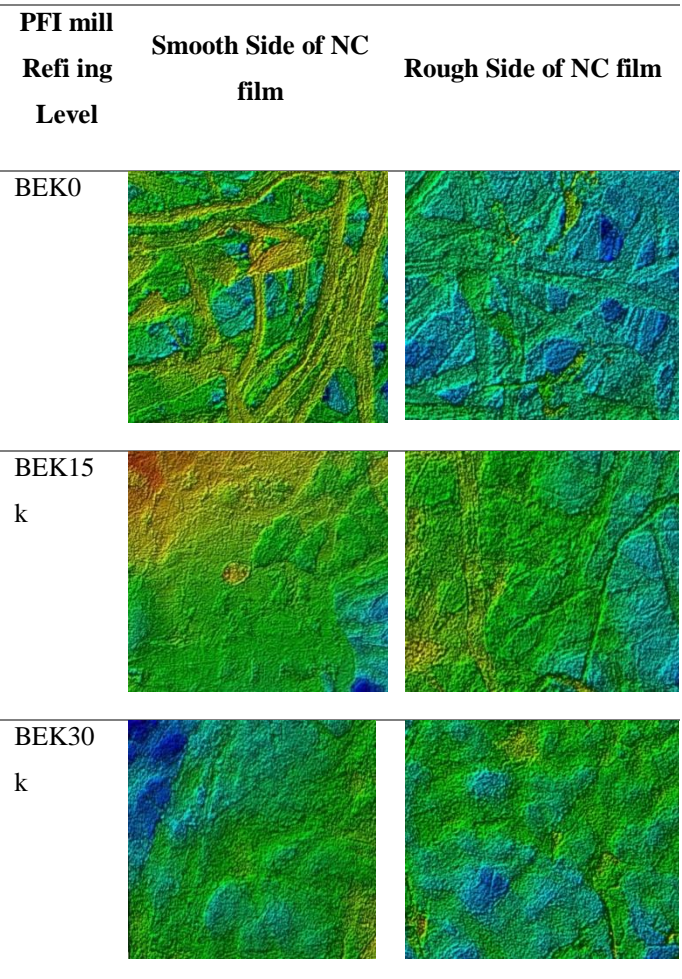


Fig S2: Surface roughness vs Refining levels for a) Disc refining b) PFI mill refining



“ENERGY EFFICIENT NANOCELLULOSE SHEETS FOR PRODUCT APPLICATION”

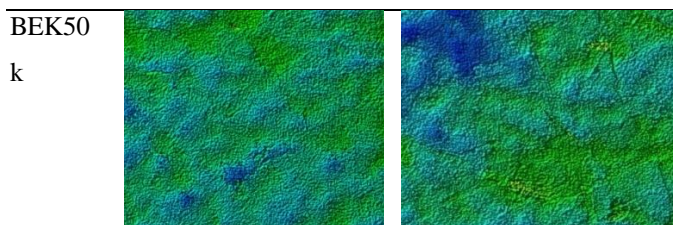


Figure S4 :Optical Profiler Images of NC sheets from Vaccum Filtration at various PFI mill refining level. 50x Magnification.

Figure S3 :Optical Profiler Images of NC sheets from Vaccum Filtration at various PFI mill refining level. 50x Magnification.

Disc Refining Level	Smooth Side of NC film	Rough Side of NC film
NBSK0		
NBSK4		
NBSK6		
NBSK11		

ENERGY EFFICIENT NANOCELLULOSE SHEETS FOR PRODUCT APPLICATION © 2022 by Wriju Kargupta is licensed under CC BY-NC-ND 4.0